Annales Geophysicae (2002) 20: 807–815 © European Geophysical Society 2002

Annales Geophysicae

Diurnal, seasonal and latitudinal variations of electron temperature measured by the SROSS C2 satellite at 500 km altitude and comparison with the IRI

P. K. Bhuyan[1], **M. Chamua**[2], **P. Subrahmanyam**[2], **and S. C. Garg**[2]

[1]Department of Physics, Dibrugarh University, Dibrugarh 786 004, India
[2]Radio and Atmospheric Science Division, National Physical Laboratory, New Dehli 110 012, India

Received: 14 June 2001 – Revised: 19 November 2001 – Accepted: 10 January 2002

Abstract. The diurnal, seasonal and latitudinal variations of electron temperature T_e, measured by the SROSS C2 satellite at equatorial and the low-latitudes during the low solar activity period of 1995–1997 are investigated. The average height of the satellite was ∼500 km and it covered the latitude belt of –31° to 34° and the longitude range of 40°–100°. T_e varies between 700–800 K during nighttime (20:00–04:00 LT), rises sharply during sunrise (04:00–06:00 LT) to reach a level of ∼3500 K within a couple of hours and then falls between 07:00–10:00 LT to a daytime average value of ∼1600 K. A secondary maximum is observed around 16:00–18:00 LT in summer. Latitudinal gradients in T_e have been observed during the morning enhancement and daytime hours. Comparison of measured and International Reference Ionosphere (IRI) predicted electron temperature reveals that the IRI predicts nighttime T_e well within ∼ 100 K of observation, but at other local times, the predicted T_e is less than that measured in all seasons.

Key words. Ionosphere, equatorial ionosphere, plasma temperature, and density

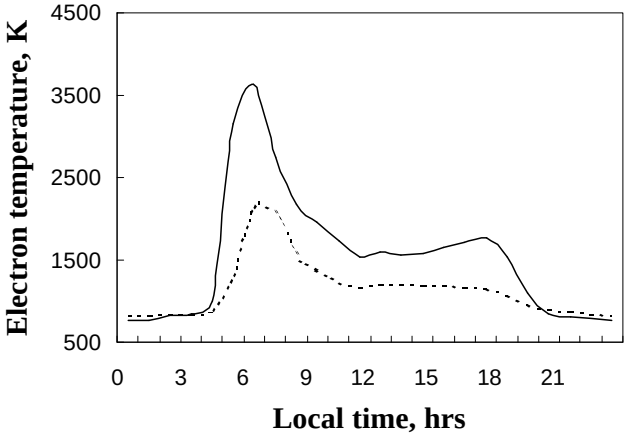

Fig. 1. Diurnal variation of observed (solid) and IRI predicted (dotted) electron temperature over the equator at ∼ 500 km.

1 Introduction

Measurement of ionospheric electron temperature gives insight into the energy balance of the ionosphere-troposphere regime. Features of electron temperature have been studied using measurements from incoherent scatter radar (McClure, 1969, 1971; Mahajan, 1977; Oliver et al., 1991), rocket probes (Oyama et al., 1980, 1996) and satellite-based instruments (Brace et al., 1967, 1988). Brace and Theis (1981) had presented empirical models of electron temperature in the ionosphere and lower plasmasphere. Richards and Torr (1986) and Watanabe et al. (1995) theoretically studied the temperature variations in the ionosphere and plasmasphere. Su et al. (1996), Oyama et al. (1996), and Balan et al. (1996 a, b) used the Sheffield University Plasmasphere Ionosphere model to investigate the temperature measurements made by the Hinotori and Exos D satellites.

The equatorial and low-latitude ionosphere exhibits many unique features in density and temperature, such as the plasma fountain, equatorial ionization anomaly, the equatorial wind and temperature anomaly, equatorial electrojet etc. The horizontal orientation of the geomagnetic field lines at the equator and the shift between the geographic and geomagnetic equator are known to be the principal reasons for observation of these features and their longitudinal variations. Though satellite-borne ionospheric experiments have been conducted in the past on satellite missions, such as Atmospheric Explorer, Dynamic Explorer, ISIS, Aeros etc., in situ measurements of the topside F-region parameters are sparse over equatorial and low-latitudes, particularly over the Indian subcontinent. The Japanese Hinotori satellite, which had a near circular orbit at 600 km, provides an ideal database for studies of temporal and spatial variations of electron density and temperature in the topside ionosphere (Watanabe and Oyama, 1995; Su et al., 1996; Oyama et al., 1996; Balan et

Correspondence to: P. K. Bhuyan (bhuyan@dibru.ernet.in)

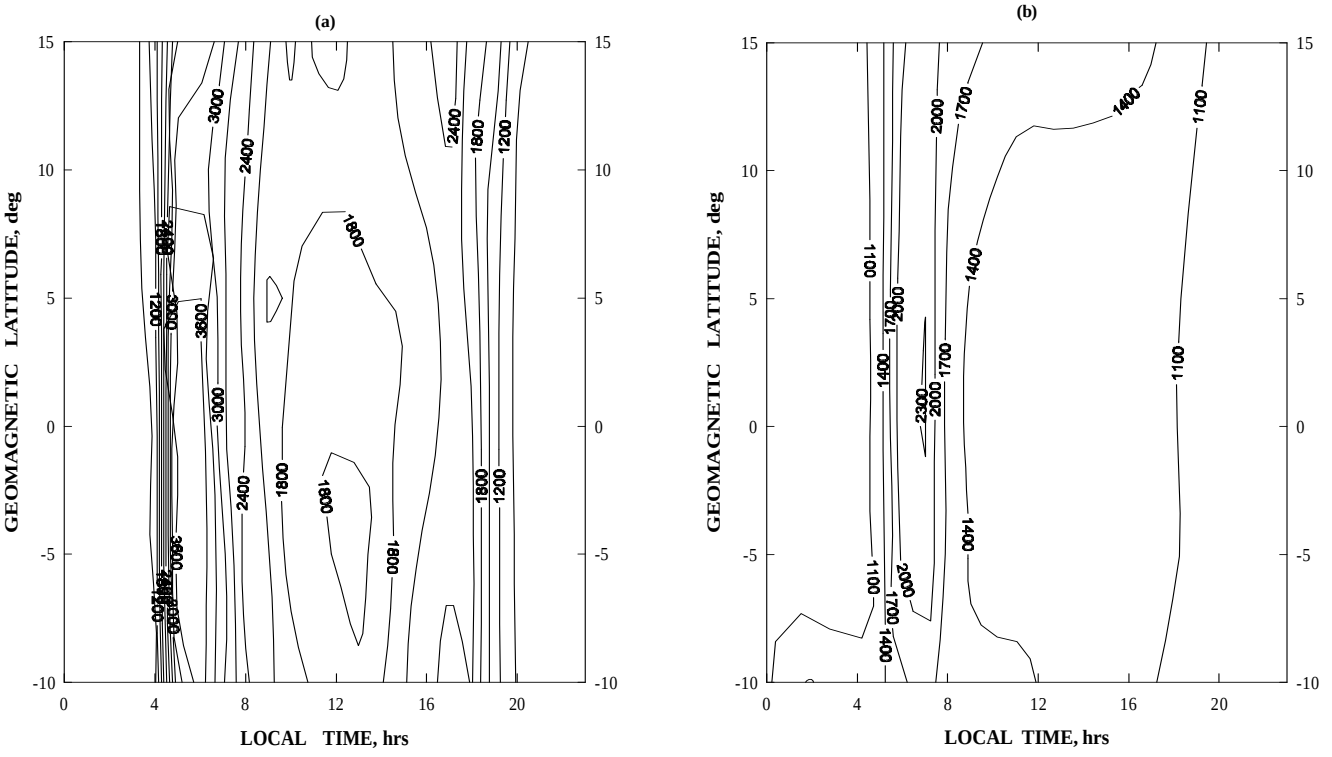

Fig. 2. Diurnal and latitudinal distribution of electron temperature at ∼500 km for **(a)** observed **(b)** IRI in northern summer.

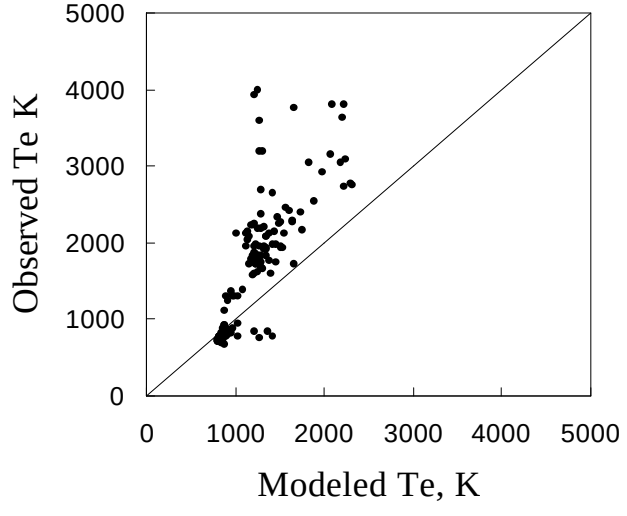

Fig. 3. Scatter plot of observed electron temperature at ∼500 km against those predicted by the IRI model for summer.

al., 1996b). But the data from the Hinotori are limited to a period of high solar activity, $150 \leq F_{10.7} \leq 220$. The SROSS C2 satellite provides an additional database for the study of electron temperature and density variations at low-latitudes under solar minimum conditions. Bhuyan et al. (2000) have earlier reported SROSS C2 density and temperature measurements at $\pm 10^{\circ}$ magnetic latitude using this database.

The aim of this study is to investigate the diurnal, seasonal and latitudinal variations of electron temperature, T_e, measured by the SROSS C2 satellite during 1995–1997. The $F_{10.7}$ cm flux corresponding to the period of observation varied between 68 and 84. The observations are also used to assess the predictability of the International Reference Ionosphere (IRI) 1995 version (Bilitza, 1990), with respect to the parameter T_e along 75°. The IRI describes the median or average values of electron density, electron content, electron temperature and ion composition as a function of height, location, local time and sunspot number for magnetically quiet conditions. It is an empirical model based on the data from the worldwide network of ionosonde stations, incoherent scatter radars (at Jicamarca, Arecibo, Millstone Hill, Malvern and St. Sanin), the ISIS and Alouette topside sounders and in situ measurements on several satellites and rockets. Results of comparison of electron temperature measurements at the low-latitude topside ionosphere with the Intercosmos 24 satellite to those predicted by the IRI have been reported by Triskova et al. (1996). Watanabe and Oyama (1995) compared the electron temperature measured by the Hinotori satellite at ∼600 km with the IRI and computer simulation results of equatorial ionosphere for high solar activity equinox conditions.

2 Instrumentation and data

The Indian satellite SROSS C2 was launched on 4 May 1994 into an orbit of 46° inclination and 930 km apogee with

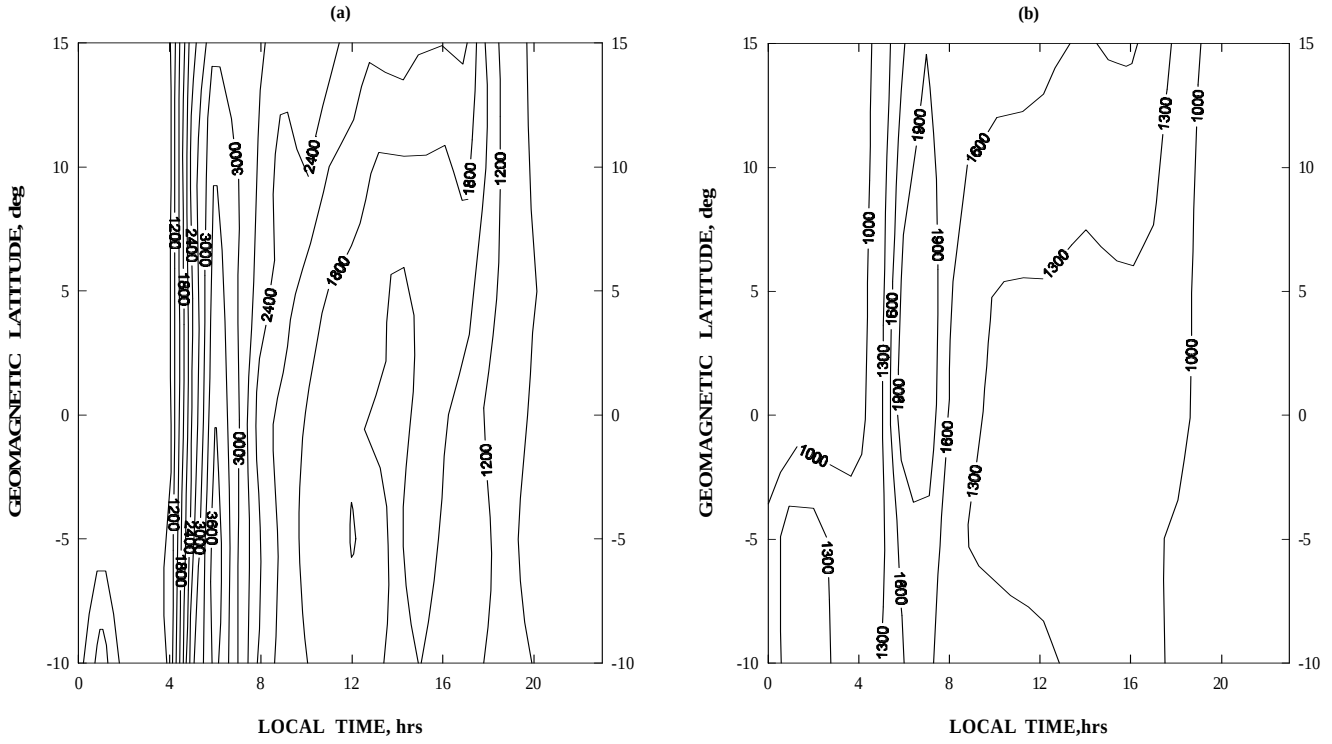

Fig. 4. Latitudinal and diurnal variation of electron temperature at ∼ 500 km for **(a)** observed **(b)** IRI in northern winter.

430 km perigee. In July 1994, the orbit of the satellite was trimmed to 630 km by 430 km. The satellite is spin stabilized with a spin rate of 5 rpm. Two Retarding Potential Analyzer (RPA) sensors were on board the satellite to measure electrons and ions separately. The RPA sensors mounted on the top deck moved in the cartwheel mode perpendicular to the spin axis of the spacecraft and collected data within 30° (for ions) and within 90° (for electrons) of the satellite's velocity vector. The data from the RPAs are transmitted to the ground station in a serial digital format at 8 kbps. The data are sampled every 22 milliseconds, which when translated into distance is ∼ 176 m, taking the satellite velocity to be 8 km/s. The RPA experiment is switched on only during the satellite visibility over the ground station at Bangalore (12.6° N, 77.3° E geographic). On average, two overhead passes lasting ∼ 10 min are tracked. The electron and ion RPA sensors consist of four grids and a collector electrode, which are mechanically identical, but are provided with different grid voltages suitable for collection of ions and electrons. The retarding grid is swept from +1.9 V to −32 V. The sensors are 120 mm in diameter and 30 mm in height with an entrance aperture of 50 mm. An annular shaped gold plated aluminium sheet of 50 mm in diameter is mounted flush on top of the sensor and connected to the satellite. The ground provides the return path for the current collected by the sensor. A least-squares fitting technique has been used to derive T_e from the slope of the linear region of the I–V characteristic curve. The ion RPA is used to derive a composite I–V curve for the ions O^+, O^2+, NO^+, H^+ and He^+ and ion density Ni (Ne) obtained from the I-V curve by fitting a nonlinear curve to the observed characteristic by the method of iteration. Garg and Das (1995) had discussed some aspects of the aeronomy experiment on SROSS C2.

3 Results

3.1 Temporal and spatial variation of T_e

The local time variations of electron temperature measured by the SROSS C2 and predicted by the IRI over the geomagnetic equator for the low solar activity ($F_{10.7}$ ∼ 75) period are shown in Fig. 1. The data were selected in the ±2.5° magnetic latitude and combined for all seasons. Measured T_e is ∼ 800 K at night and ∼1600 K at noon. Enhancement in T_e up to ∼ 3500 K occurs in the morning between 04:00–06:00 LT. An afternoon increase of lower amplitude is also observed between 16:00–18:00 LT. The nighttime T_e predicted by the IRI is ∼800 K and at noon it is ∼ 1200 K. The morning enhancement reaches a level of ∼ 2000 K and no afternoon increase is predicted by the IRI. The measured electron temperature for northern summer months (May, June, July, and August) is plotted in a local time (00:00–23:00) versus magnetic latitude (−10° to 15°) grid and shown in Fig. 2a. All the data are grouped into bins of 5° in latitude and 1 h in local time. The groupings in latitude and local time are aimed at minimizing any error that may be introduced due to a lack of adequate data. Data beyond −10° have not been considered for the study due to the same rea-

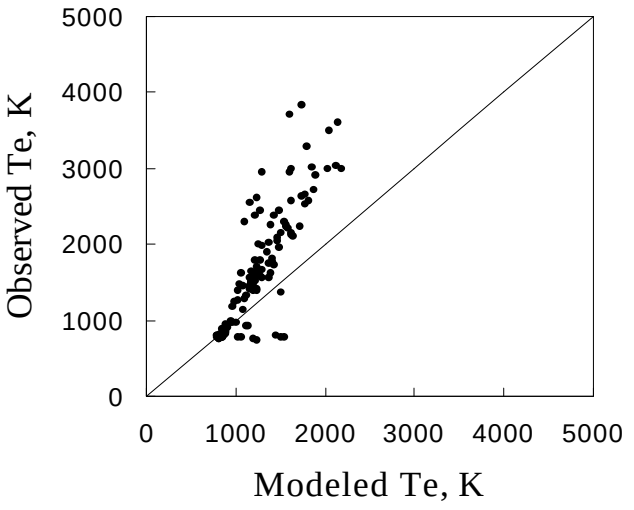

Fig. 5. Scatter plot of observed electron temperature at ∼500 km versus electron temperature predicted by IRI for winter.

son. Consequently, each data point is an average of 15 to 20 values or more. The maximum error in T_e is ∼ ±5% of the observed value within the limits 500 K to 5000 K. T_e varies between 700 K to 800 K during nighttime (20:00–04:00 LT), rises sharply during sunrise (04:00–06:00 LT) to reach a level of 3500 K and above within a couple of hours and then falls between 07:00–10:00 LT to a daytime average value of ∼1600 K. A secondary maximum is observed in this season between 16:00–18:00 LT. The amplitude of the morning enhancement in T_e is higher at latitudes south of the equator, while the amplitude of the afternoon peak is greater at northern latitudes. The difference in peak morning temperature between the southern and northern latitudes is 900 K and the difference in the evening enhancement between northern and southern latitudes is 400 K. Daytime T_e shows a gradual increase from south to north. Nighttime values of electron temperature are about equal at all latitudes. The ratio between day and nighttime T_e varies between 2.1 and 2.9. Observation with the Hinotori satellite (Oyama et al., 1996) within ±31° at ∼600 km during periods of moderate ($F_{10.7}$ ∼150) and high ($F_{10.7}$ ∼230) solar activity shows that average T_e during nighttime is ∼1050 K and ∼1260 K and during daytime, average T_e is ∼1550 K and ∼1880 K, respectively. The peak morning temperature observed during moderate and high solar activity was ∼4200 K and ∼5000 K, respectively. Since an altitude difference of 100 km is not expected to appreciably change the electron temperature in the topside ionosphere, the electron temperature measured by the SROSS C2 during solar minimum is lower than that measured by the Hinotori in moderate and high activity periods at all local times.

The diurnal and latitudinal variations of T_e predicted by the IRI at 500 km for the same space time configuration as in case of observed T_e for summer is shown in Fig. 2b. Comparison of the two figures reveals that IRI predicts nighttime T_e well within ∼100 K of observation, but underestimates it during the daytime at all latitudes. The morning enhancement in temperature predicted by the IRI shows a peak around the equator, but contrary to observation, no secondary enhancement in the afternoon hours has been predicted. Oyama (1994) reported that the morning enhancement of T_e is reproduced in the IRI only up to about 500 km and is absent at higher altitudes. The difference between measured and predicted T_e in summer is further illustrated in Fig. 3, where observed T_e is plotted against computed T_e for all local times and latitudes. The model underestimates T_e in the morning enhancement period by as much as 50% to 70%. The deviation between the two sets increases for higher temperatures.

Figure 4a illustrates the diurnal and latitudinal variations of observed electron temperature in northern winter (November, December, January and February). In winter, the rise in morning T_e is rather slow at all latitudes compared to that in summer. The peak enhancement gradually decreases from south to north. The difference in peak morning temperature between the Southern and Northern Hemisphere is 800 K. The fall in electron temperature after the peak is gradual throughout the day. The nighttime T_e is ∼800 K in this season. Daytime T_e is higher (∼2200 K) at northern latitudes than that observed at southern latitudes (∼1500 K). In Fig. 4b, the diurnal and latitudinal variations of the IRI predicted T_e are shown. Comparison of Figs. 4a and b shows that IRI predicts nighttime T_e almost accurately, but gives lower values of daytime T_e. The difference between predicted and observed T_e in the morning hours is ∼40%. The predicted electron temperature during noon decreases from a high value in the south to a low value in the north, as in the case of measured T_e. The IRI predicted T_e is ∼20% lower than that observed during these hours. Deviation of the predicted electron temperature in winter from that observed is further illustrated in the scatter plot (Fig. 5) between the two sets. It is seen that about all values greater than ∼1000 K, i.e. all daytime observed T_e are higher than those predicted by the IRI.

The temporal and spatial variations of observed and IRI predicted T_e, in the months of March, April, September and October (equinoxes) are shown in Fig. 6a and Fig. 6b, respectively. Measured nighttime T_e is ∼800 K at all locations. The morning enhancement begins earlier (03:00 LT) at southern latitudes than at northern latitudes (04:00 LT). The rate of increase of T_e is faster in equinox and summer compared to that in winter. Observed electron temperature remains at the peak level for about 2 h (05:00–07:00 LT) and then decreases slowly to reach the daytime level of ∼1600 K in the south and ∼2000 K in the north. The amplitude of the morning enhancement is higher (∼3500 K) at the equator as compared to that at higher latitudes, either north (∼2800 K) or south (∼3200 K). The ratio of daytime to nighttime T_e varies between 2 and 2.5. As seen in summer and winter, IRI predicts nighttime T_e well in the equinoxes. But at other local times, predicted T_e is lower than that observed. The difference between observation and prediction could be as high as ∼40% in the morning hours and ∼25% in the daytime.

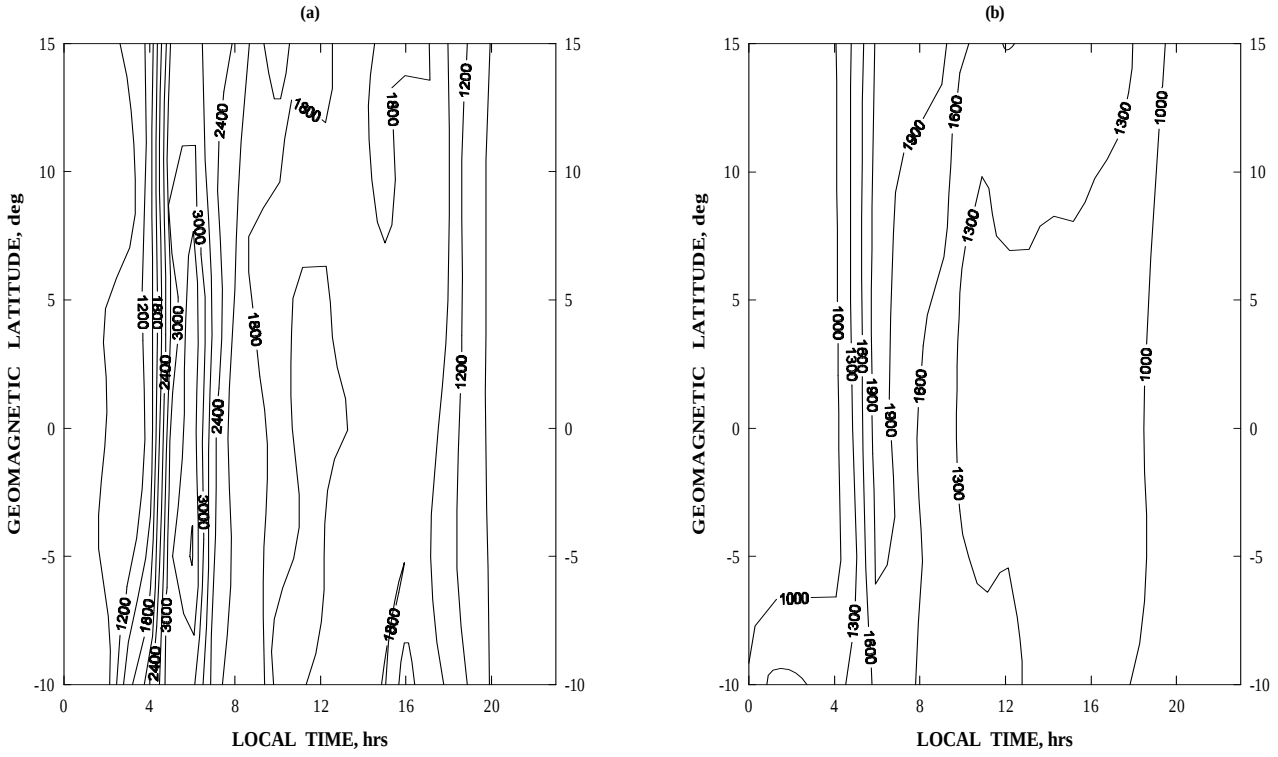

Fig. 6. Latitudinal and diurnal variations of electron temperature at ∼ 500 km for **(a)** observed and **(b)** IRI in the equinoxes.

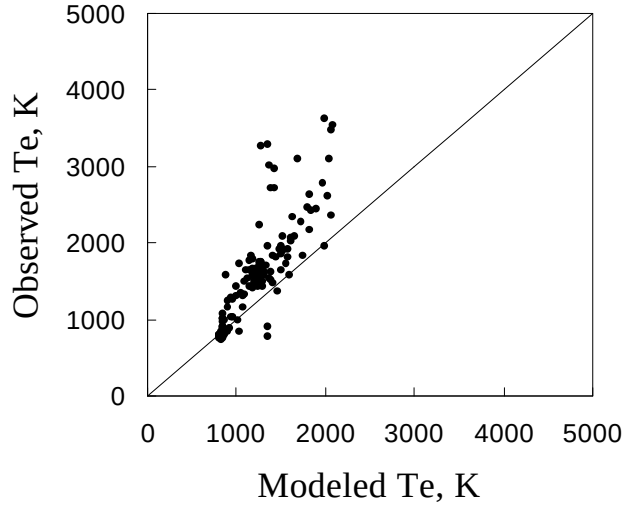

Fig. 7. Scatter plot of observed electron temperature at ∼ 500 km against the temperature predicted by the IRI model for equinoxes.

Figure 7 shows the deviation between the two data sets at all local times and latitudes.

3.2 Electron temperature and electron density

The latitudinal variation of T_e measured at the 500 km altitude at selected hours of the day is shown in Fig. 8 for the three seasons. It may be noted that during the morning enhancement, electron temperature is higher at latitudes south of the equator and decreases towards northern mid-latitudes. The decrease from the equator to the north is faster in the June solstice and equinoxes compared to that in the December solstice. At 10:00 LT and 14:00 LT, electron temperature is minimum near or south of the equator and increases towards the north. The increase in temperature with latitude is faster in the December solstice. In the June solstice, electron temperature observed at 18:00 LT is higher than or nearly equal to the daytime temperatures. The latitudinal variation of electron density at the selected hours seen in the right-hand panel of Fig. 8 shows that during the daytime hours, density is higher near or south of the equator and lower at latitudes greater than 5° N. At 06:00 LT, the density increases from south towards north. The inverse variation of electron density with latitude in the daytime and morning hours appears to have a direct bearing on the mirror image similar to the behavior of electron temperature seen in its latitudinal variation. The relationship between SROSS C2 measured electron temperature and electron density is further illustrated in Fig. 9 for all data in the corresponding season. It is seen that temperature decreases with an increase in density in all seasons for T_e above the level of 1000 K. Thus, nighttime T_e is independent of density, whereas an inverse relationship exists between the two during the daytime. The increase in amplitude of the morning enhancement has been observed during moderate and high solar activity period by Oyama et al. (1996). They also found a correlation between an increase in morning temperature and a decrease in electron density. Ma-

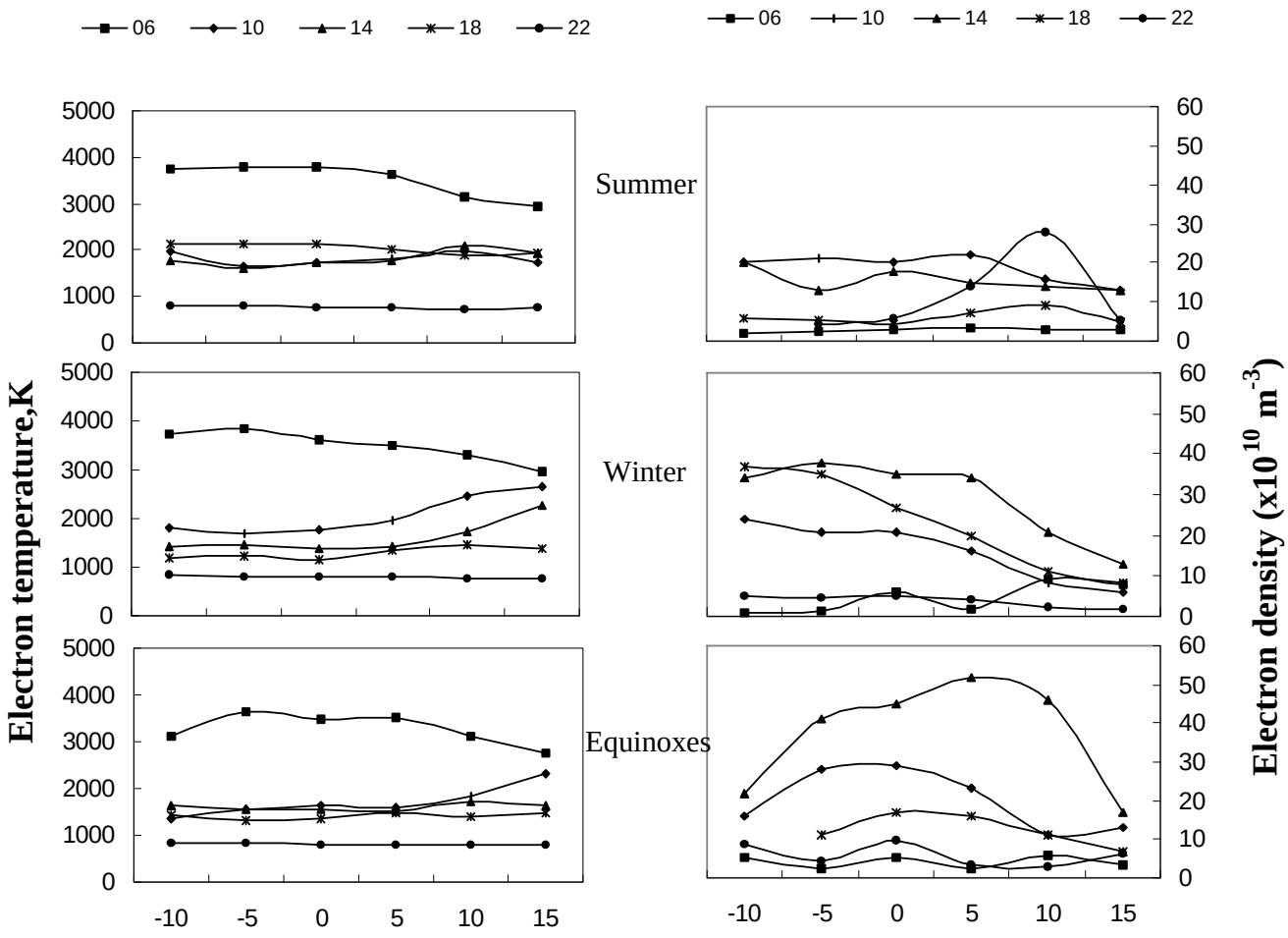

Fig. 8. Latitudinal variation of observed electron temperature (left panels) and electron density (right panels) at selected local times.

hajan (1996) reported a linear negative relationship between T_e and Ni measured by the Arecibo radar during a period of low solar activity ($F_{10.7} = 75$). He observed that this relationship is valid only for the limited region of the ionosphere below 300 km at low-latitude, where local equilibrium between electron heating and cooling rates exists. At higher altitudes (> 400 km), thermal conduction becomes the major controlling factor of T_e due to heat conducted down from the protonosphere along magnetic field lines. On the other hand, Brace and Theis (1978) reported from a study of electron temperature and density measured by the Atmospheric Explorer C satellite during December 1973–December 1974, a period of low solar activity at altitudes below 200 km, where the electrons are primarily cooled by collision with neutrals; the electron temperature was nearly independent of plasma density, with both parameters increasing with altitude. At higher altitudes, where electrons are increasingly cooled by collisions with ions, the temperature and density begins to exhibit an inverse relationship. This relationship was found to be the same over a wide range of latitudes, longitudes and seasons, which allows for an estimation of electron temperature wherever plasma density measurements from other sources are available. Present observation indicates that the equilibrium between electron heating and cooling rates extends up to the height of 500 km in Indian low-latitudes during the daytime.

Electron temperature observed during the period 1995–1997 by the SROSS C2 satellite shows large day-to-day variability. Figure 10 shows an example of the variability of T_e in the three seasons at the magnetic equator. The variability of electron temperature from one day to another may be attributed to the variability in electron density, since the heat input to the electron gas is not expected to change from one day to the next as long as solar activity is constant. The electron density, however, could vary from day-to-day due to changes in ion drift and in the case of satellite observation, due to spatial variations. Since the heat that is lost by the electrons to the ions depends upon the ion (electron) density, the temperature of the electron gas is likely to be controlled by electron density. Electron density measurements of the corresponding period also show large day-to-day variability in all seasons.

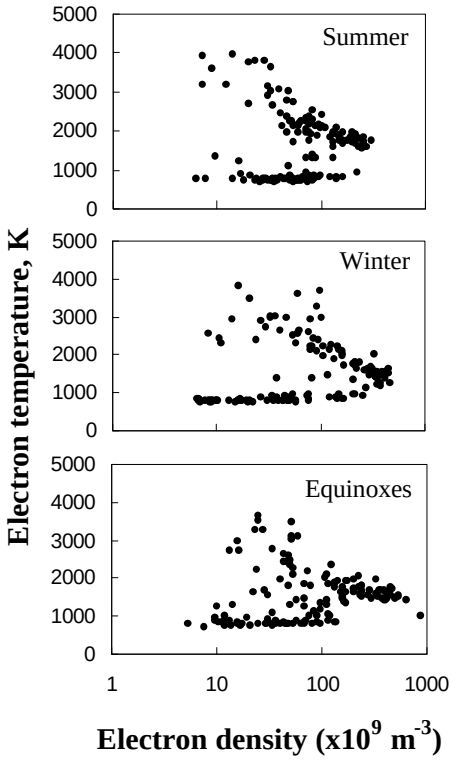

Fig. 9. Variation of observed electron temperature (all data) with the observed electron density in the corresponding seasons.

4 Summary and Discussion

In the F-region, the photoelectron produced by solar EUV radiation heats the ambient electrons. The heat energy of the ambient electrons is lost to both the ions and neutral particles that surround the electrons. The balance between heating, cooling and energy flow processes, therefore, determines the electron temperature in the F-region of the ionosphere. The electron energy equation in the F-region in absence of field-aligned currents may be written as (Schunk and Nagy, 1978):

$$\frac{3}{2}N_e k\frac{\partial T_e}{\partial t} = \sin^2 I\frac{\partial}{\partial z}\left(K^e\frac{\partial T_e}{\partial z}\right) + \sum Q_e - \sum L_e, \quad (1)$$

where z is the vertical height, I is the geomagnetic dip angle, N_e and T_e are the electron density and electron temperature, respectively, k is the Boltzman's constant, K^e is the electron thermal conductivity, Q_e and L_e are the heating and cooling rates, respectively. Most of this energy is deposited through ionization of O and N_2, which are the principal species at F2 region altitudes, and intense heating of the ionosphere takes place due to photoionization. The photoelectrons rapidly thermalize through a number of energy loss mechanisms, including ionization of the neutral species by the very energetic primary electrons, electronic excitation of O and O_2, vibrational excitation of N_2, and rotational excitation of O_2 and N_2. At high altitudes, Coulomb scattering by ambient electrons and elastic collision with neutrals and ions are important loss processes. At energies of the order of 20 to 50 eV, the principal mechanism is excitation of neutral species. At energies of a few to $\sim$20 eV, excitation of O, O_2 and N_2 is more significant. At still lower energies, vibrational excitation of N_2 is the principal mode of energy loss in the range 2 eV to 4 eV. Finally, at thermal energies, inelastic collisions with N_2 and O are dominant energy loss mechanisms. Electron-electron collision through Coulomb interaction constitutes the most efficient means of energy removal for electrons below $\sim$30 eV. The electron energy is also spatially redistributed by heat conduction (Whitten and Poppoff, 1971).

The electron temperature increases by more than 2500 K from its nighttime value in the post sunrise hour. Dalgarno and McElory (1965) first predicted the rapid increase in T_e in the early morning hours. DaRosa (1966) calculated the time dependent behavior of T_e during morning hours. Experimental evidence of the morning enhancement has also been reported (Evans, 1965; McClure, 1971; Clark et al., 1972). Oyama et al. (1996) reported that electron temperature in the morning rises from about 1200 K to about 4000 K within $\pm 30^\circ$ magnetic latitude. They observed that the morning enhancement is strong during northern summer months and grows with an increase in solar activity. Enhancement in morning T_e is due to photoelectron heating. Photoelectron production begins at sunrise through the ionization of neutral particles. As the photoelectrons share their high energy with the ambient electrons, the electron temperature increases, where the increase is rapid in the early morning hours due to low electron density. From theoretical simulation of observed T_e enhancements, Oyama et al. (1996) have shown that intense morning enhancement of T_e observed over the equator is due to reduction in electron density caused by the downward drift of plasma, which usually occurs in the morning hours. After sunrise, temperature decreases as electron density increases and energy is shared between more electrons. The daytime valley is the result of the balance between electron heating and cooling processes. Though near-noon electron heating by solar EUV is maximum, it is more than offset by electron cooling, resulting from the higher noontime electron density. The latitudinal variation of morning and daytime electron temperatures is influenced by the latitudinal variation of electron density. The electron temperature also increases in the afternoon in the same way as in the morning of a June solstice. Watanabe and Oyama (1996) have reported enhancement of electron temperature at $\sim$18:00 LT in the mid-latitudes from measurements of the Hinotori satellite during 1981–1982. From a three-dimensional computer simulation carried out to study the measurements made by the Hinotori satellite, Watanabe et al. (1995) have found that the afternoon enhancement in the mid-latitudes comes from the balance of heating and cooling. The enhancement is influenced by meridional neutral wind. Around the equatorial anomaly region, the electron temperature in the topside F-region increases in the evening due to the competing effects of plasma cooling and plasma transport. Downward $\boldsymbol{E} \times \boldsymbol{B}$ drift near sunset can carry the

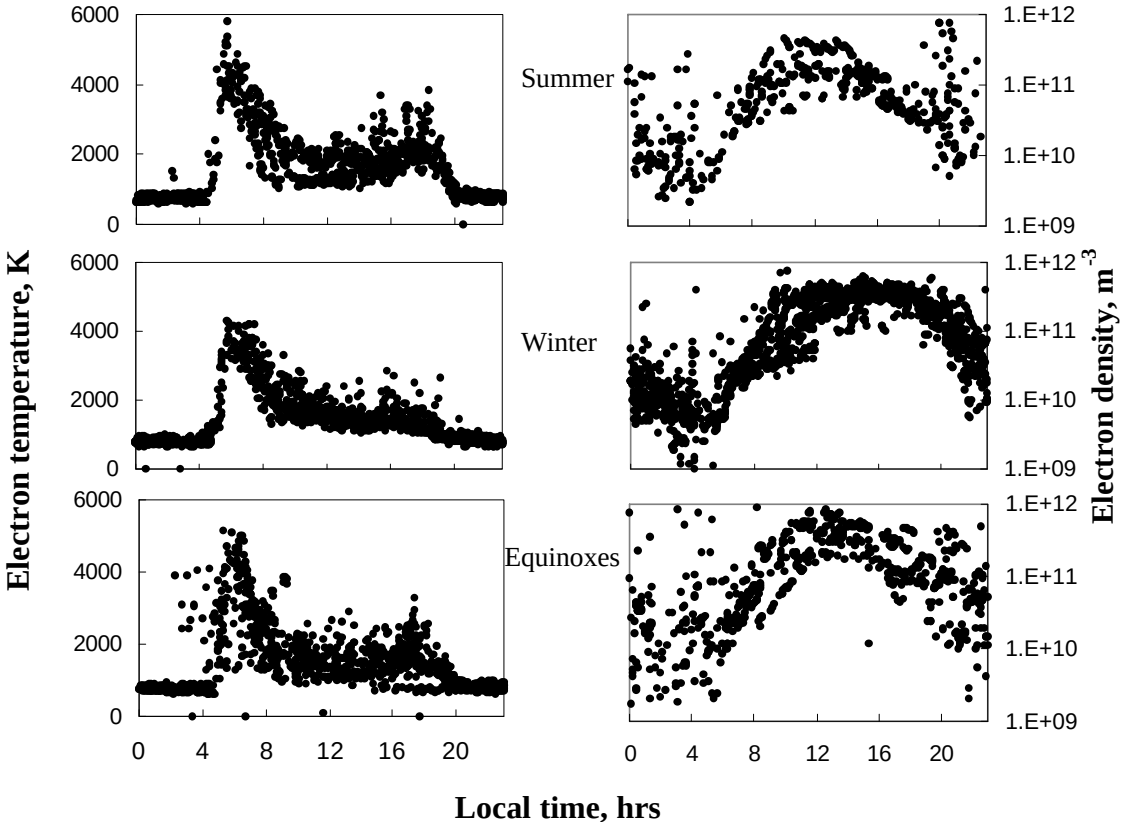

Fig. 10. Diurnal variation of electron temperature (left column) and electron density (right column) at the magic equator during 1995–1997.

high altitude dayside hot plasma into the topside F-region, leading to the observed enhancement of electron temperature.

5 Conclusion

Plasma temperature measurements were carried out with the SROSS C2 satellite during the low solar activity period of 1995–1997 in the 75° Indian longitude sector. The electron temperature at 500 km is ∼800 K during nighttime, increasing to a level of ∼3500 K at sunrise and then settling down to a daytime average value of ∼1600 K within a couple of hours after sunrise. A secondary enhancement in the afternoon hours of the summer months has also been observed. The ratio between day and nighttime electron temperatures varies from 2.1 to 2.9. A north/south difference in the peak morning enhancement and in the daytime temperature was observed. The IRI predicts the nighttime temperature within 100 K of observation, but during the morning enhancement and, daytime predicted, temperature is found to be less than that measured by the satellite.

Acknowledgement. This work is partially supported by the Indian Space Research Organization through a grant (SROSS C2/ph2/99). The authors wish to thank the NASA, USA for making the IRI-1995 available through the Internet. The authors are also thankful to all associated with the SROSS C2 data acquisition program.

Topical Editor M. Lester thanks K. Oyama and another referee for their help in evaluating this paper.

References

Balan, N., Oyama, K. I., Bailey, G. J., and Abe, T.: Plasmasphere electron temperature studies using satellite observations and a theoretical model, J. Geophys. Res., 101, 15 323–15 330, 1996a.

Balan, N., Oyama, K. I., Bailey, G. J., and Abe, T.: Plasmasphere electron temperature profiles and the effects of photoelectron trapping and an equatorial high-altitude heat source, J. Geophys. Res., 101, 21 689–21 696, 1996b.

Bhuyan, P. K., Kakoty, P. K., Garg, S. C., and Subrahmanyam, P.: Observation of electron and ion temperature and electron density at ±10° magnetic latitude from SROSS C2 measurements over India and comparison with the IRI, (Communicated to J. Atmos. Solar Terr. Phys.), 2000.

Bilitza, D.: International Reference Ionosphere-1990 NSSDC 90–22, World Data Center A, Rockets and Satellites, Greenbelt, Md, USA, 1990.

Brace, L. H., Reddy, B. M., and Mayr, H. G.: Global behaviour of the ionosphere at 1000 kilometre altitude, J. Geophys. Res., 72, 265–283, 1967.

Brace, L. H. and Theis, R. F.: An empirical model of the interrelationship of electron temperature and density in the daytime thermosphere at solar minimum, Geophys. Res. Lett., 5, 275–281, 1978.

Brace, L. H. and Theis, R. F.: Global empirical models of ionospheric electron temperature in the upper F-region and plasmasphere based on in situ measurements from the Atmospheric Explorer-C, ISIS-1 and ISIS-2 satellites, J. Atmos. Terr. Phys., 43, 1317–1343, 1981.

Brace, L. H., Chapell, C. R., Chandler, H. O., Comfort, R. H., Horwitz, J. L., and Hoegy, W. R.: F-region electron temperature signatures of the plasmapause band on Dynamic explorer 1 and 2 measurements, J. Geophys. Res., 93, 1896–1908, 1988.

Clark, D. H., Raitt, W. J., and Willmore, A. P.: The global morphology of electron temperature in topside ionosphere as measured by ac Langmuir probe, J. Atmos. Terr. Phys., 34, 1865–1880, 1972.

Dalgarno, A. and McElory, H. B.: Ionosphere electron temperature near dawn, Planet. Space Sci., 13, 143–145, 1965.

DaRosa, A. V.: The theoretical time dependent thermal behaviour of the ionosphere electron gas, J. Geophys. Res., 71, 4107–4120, 1966.

Evans, J. V.: Cause of the mid-latitude evening increase in foF2, J. Geophys. Res., 70, 1175–1185, 1965.

Garg, S. C. and Das, U. N.: Aeronomy experiment on SROSS-C2, J.Spacecraft Technology, 5, 11–15, 1995.

Mahajan, K. K.: Models of electron temperature in the ionospheric F-region using electron density height profiles, J. Atmos. Terr. Phys., 39, 637–639, 1977.

Mahajan, K. K.: Contributions of incoherent-scatter radar measurements at Arecibo for the improvement of IRI, Adv. Space Res., 18, 131–134, 1996.

McClure, J. P.: Diurnal variation of neutral and charged particle temperatures in the equatorial F-region, J. Atmos. Terr. Phys., 74, 279–291, 1969.

McClure, J. P.: Thermospheric temperature variation inferred from incoherent scatter observations, J. Geophys. Res., 76, 3106–3115, 1971.

Oliver, W. M., Takami T., Fukao, S., Sato T., Yamamoto, M., Thuda, T., Nakamura, T., and Kato, S.: Measurement of ionospheric and thermospheric temperatures and densities with the Middle and Upper Atmosphere radar, J. Geophys. Res., 96, 17 827–17 838, 1991.

Oyama, K. I., Hirao, K., Banks, P. M., and Williamson, P. R.: Is T_e equal to T_n at the heights of 100–120 km?, Planet. Space Sci., 28, 207–211, 1980.

Oyama, K. I.: Verification of IRI plasma temperature of great altitude by satellite data, Adv. Space Res., 14, 105–113, 1994.

Oyama, K. I., Balan, N., Watanabe, S., Takahashi, T., Isoda, F., Bailey, G. J., and Oya, H.: Morning overshoot of T_e enhanced by downward plasma drift in the equatorial topside ionosphere, J. Geomag. Geoelec., 48, 959–966, 1996.

Rajaram, G.: Structure of the equatorial F-region topside and bottomside-A review, J. Atmos. Terr. Phys., 39, 1125–1144, 1977.

Richards, P. G. and Torr, D. G.: Thermal coupling of conjugate ionosphere and the tilt of the Earth's magnetic field, J. Geophys. Res., 91, 9017–9025, 1986.

Schunk, R. W. and Nagy, A. F.: Electron temperatures in the F-region of the ionosphere: Theory and observation, Reviews of Geophys., 16, 355–399, 1978.

Stening, R. J.: Modeling the low-latitude F-region, J. Atmos. Terr. Phys., 54, 1387–1412, 1992.

Su, Y. Z., Oyama, K. I., Bailey, G. J., Takahashi, T., and Watanabe, S.: Spatial and temporal variations of the electron temperature at equatorial anomaly latitudes, Adv. Space Res., 18, 83–86, 1996.

Triskova, L., Smilaver, J., Truhlik, V., and Afonon, V. V.: On the low-latitude topside models: II. Electron temperature, Adv. Space Res., 18, 213–216, 1996.

Watanabe, S. and Oyama, K. I.: Dynamic Model and Observation of the Equatorial Ionosphere, Adv. Space Res., 15, 109–112, 1995.

Watanabe, S., Oyama, K. I., and Abdu, M. A.: Computer simulation of electron and ion densities and temperatures in the equatorial F-region and comparison with Hinotori results, J. Geophys. Res., 100, 14 581–14 590, 1995.

Watanabe, S. and Oyama, K. I.: Effects of neutral wind on the electron temperature at a height of 600 km in the low-latitude region, Ann. Geophysicae, 14, 290–296, 1996.

Whitten, R. C. and Poppoff, I. G.: Fundamentals of aeronomy, John Wiley & Sons, Inc. 1971.